Supplementary Animation **http://www.seevccc.rs/HLDpaper/NMMB_DREAM_circumpolar_dustload_animation.gif**

Table S1. The contemporary category of the newly identified high latitude dust sources included in this study, based on the currently available observations. The number refers to the source number in the map of Figure 1. In addition, McMurdo Dry Valley is estimated to best fit to Category 3 and the McMurdo Ice shelf 'debris bands' to Category 2.

Cat	HLD No.	Description	Climatic or environmental significance	Criteria
1	30, 31, 32, 34	Active source	High	Frequently active dust source with >10 dust events documented
2	25, 26, 27, 35	Moderately active source	Moderate	5-10 dust events documented or a smaller potential source area
3	1, 2-24, 28-29, 33, 36-64	Source with unknown activity	Small/Currently unknown	Infrequent activity or a new source with 1-5 dust events documented

Table S2. Iceland dust sources and observations on dust events identified in this study based on in satellite images of 2002-2011.

Location in Iceland	Satellite observations
No. 23 Reykjanes	2 events, 2004 and 2011
No. 24 Eyrabakki	3 events, 2002-2011
No. 25 Hagavatnssvæði	8 events, 2002-2011
No. 26 Fljótshlíð	8 events, 2002-2011
No. 27 Langisjór	5 events in 2010; 3 events in 2002-2011
No. 28 Eldhraun/Landbrot	3 events 2002-2011
No. 29 Eldhraun	3 events 2002-2011
No. 30 Klausturfjara	17 events 2002-2011
No. 31 Núpsvötn	39 events 2002-2011
No. 32 Holuhraun	29 events 2002-2011
No. 33 Vikurhraun/Vikursandur	2 events 2002-2011
No. 34 Höfn í Hornarfirði	13 events 2002-2011
No. 35 Lónsvík	8 events 2002-2011

20

Table S3. West coast of Greenland observations for the new dust sources identified for the first time in this study (No. 53-58), based on satellite observations from 2021, and earlier satellite observations for sources identified in East Greenland and Canada (No. 59-64), north of 70 ºN.

Latitude	Longitude	No.	Description	Dust example	Observed events
63.5059	-51.0454	53	West coast of Greenland, the source appears to be in the delta area, not in the valley	https://go.nasa.gov/3biOSt9	26 Oct 2021
62.2421	-49.0481	54	West coast of Greenland, the source appears to be a small valley with a glacier	https://go.nasa.gov/3Gw80SV	23/25 Oct 2021
63.5163	-50.9652	55	West coast of Greenland, source appears to be the delta area (Sentinel shows dust plumes up 10 km from the coast, east of delta)	https://go.nasa.gov/3Ct5cmY	18,19,25,26 Oct 2021
65.7621	-51.2866	56	West coast of Greenland, a very narrow valley (not clear if dust comes from the valley or termination tip of glacier). Clear dust plumes when flipping images Aqua/Terra	https://go.nasa.gov/2ZBLvv2	18 and 22 Oct 2021
62.4791	-50.2146	57	West coast of Greenland, small trip of land between sea and glacier	https://go.nasa.gov/2ZyWbea	18 Oct 2021
67.359	-52.3693	58	West coast of Greenland, a short valley, several dust clouds appear	https://go.nasa.gov/3vU4qwR	18 Oct 2021
71.8288	-22.8017	59	East Greenland	https://go.nasa.gov/3pOPjnq	3 Oct 2019
70.4565	-22.2694	60	East Greenland	https://go.nasa.gov/3Gx1paM	15 Sep 2020
78.0407	-21.4572	61	East Greenland	https://go.nasa.gov/3Gw4g3R	24 Sep 2003
81.3073	-78.2145	62	Canada	https://go.nasa.gov/3mxJxEZ	2 July 2020
71.8426	-22.7902	63	East Greenland, better seen in S2 and L8	https://go.nasa.gov/3Bt9jy2	30 Sept 2018
72.3906	-25.1555	64	East Greenland	https://go.nasa.gov/3vXOWb6	23 Sep 2003

Table S4. Locations of the HLD sources and G-SDS-SBM source intensity (SI) values at location and maximum values find in certain environment given location (areas within the distance from location of 30 arcsec, 0.1°, 0.5° and 1°); SI is undefined (-99.0) if location mark is not over land; area south of 60°S is not included in G-SDS-SBM and values at locations in this area are marked with a dash.

No.	lat	lon	at loc.		30 arcsec		0.1°		0.5°		1°	
			max	min	max	min	max	min	max	min	max	min
1	57.6482	10.4059	0.8	0.0	0.9	0.0	1.0	0.0	1.0	1.0	1.0	1.0
2	63.2	75.5	0.1	0.0	0.1	0.0	0.1	0.0	0.3	0.2	0.5	0.2
3	60.1	71.4	0.0	0.0	0.0	0.0	0.3	0.0	0.3	0.0	0.8	0.3
4	58.9	69.2	0.0	0.0	0.0	0.0	0.2	0.0	0.7	0.3	0.8	0.3
5	56.5	67.5	0.1	0.0	0.2	0.0	0.2	0.0	0.3	0.1	0.5	0.1
6	67.6	33.4	0.0	0.0	0.0	0.0	0.8	0.0	0.9	0.0	1.0	0.0
7	51.3	88.5	0.0	0.0	0.0	0.0	0.2	0.0	0.4	0.0	0.4	0.2
8	47.3	66.7	0.5	0.0	0.5	0.0	0.6	0.3	0.7	0.4	1.0	0.7
9	-77.9	165.2	-	-	-	-	-	-	-	-	-	-
10	63.5	-18.2	1.0	0.0	1.0	0.0	1.0	1.0	1.0	1.0	1.0	1.0
11	71.4	128.5	0.0	0.0	0.3	0.0	0.4	0.0	1.0	0.0	1.0	0.0
12	81.7	-71.1	0.7	0.0	0.8	0.0	1.0	0.0	1.0	0.0	1.0	0.0
13	77	16	-99.0	-99.0	-99.0	-99.0	0.9	0.0	1.0	0.0	1.0	0.0
14	60.5	-144.9	0.6	0.0	0.9	0.0	1.0	0.0	1.0	0.5	1.0	0.5
15	56.0054	8.1138	0.0	0.0	0.9	0.0	1.0	0.0	1.0	1.0	1.0	1.0
16	69.36	-123.97	0.7	0.0	1.0	0.0	1.0	0.0	1.0	0.0	1.0	0.0
17	-45.48	-68.78	0.0	0.0	0.7	0.7	0.8	0.7	0.9	0.8	0.9	0.8
18	77	15	-99.0	-99.0	-99.0	-99.0	1.0	0.0	1.0	0.0	1.0	0.0
19	-63.9	-57.9	-	-	-	-	-	-	-	-	-	-
20	-64.2	-56.6	-	-	-	-	-	-	-	-	-	-
21	70.4	-52.5	0.5	0.0	0.6	0.0	0.8	0.0	1.0	0.0	1.0	0.0
22	78.7	15.7	0.3	0.0	0.3	0.0	0.7	0.0	1.0	0.0	1.0	0.0
23	63.85	-22.21635	0.0	0.0	0.7	0.1	1.0	0.9	1.0	1.0	1.0	1.0
24	63.87	-21.18885	0.0	0.0	1.0	0.0	1.0	0.0	1.0	1.0	1.0	1.0
25	64.47	-20.32702	0.4	0.0	0.4	0.0	0.6	0.2	0.8	0.5	1.0	1.0
26	63.72	-20.14013	0.2	0.0	0.2	0.0	0.3	0.1	1.0	1.0	1.0	1.0
27	64.14	-18.29022	0.3	0.0	0.3	0.0	0.4	0.0	0.9	0.7	1.0	1.0
28	63.69	-18.20012	0.0	0.0	0.4	0.0	1.0	1.0	1.0	1.0	1.0	1.0
29	64.03	-17.99276	0.0	0.0	0.2	0.0	0.3	0.0	1.0	1.0	1.0	1.0

30	63.7	-17.75925	0.9	0.0	0.9	0.0	1.0	0.7	1.0	1.0	1.0	1.0
31	63.91	-17.54640	0.6	0.0	0.6	0.5	1.0	0.5	1.0	1.0	1.0	1.0
32	64.84	-16.84550	0.2	0.0	0.3	0.0	0.5	0.0	0.5	0.0	1.0	1.0
33	65.02	-16.49492	0.0	0.0	0.2	0.0	0.5	0.0	0.6	0.3	1.0	1.0
34	64.24	-15.21443	0.0	0.0	0.0	0.0	1.0	0.1	1.0	1.0	1.0	1.0
35	64.38	-14.76743	0.3	0.0	0.7	0.0	1.0	1.0	1.0	1.0	1.0	1.0
36	-45.56	-68.7378	0.0	0.0	0.7	0.6	0.8	0.7	0.9	0.8	0.9	0.9
37	-53.217	-68.6934	0.0	0.0	0.3	0.2	1.0	0.9	1.0	1.0	1.0	1.0
38	-53.78	-67.8064	0.9	0.0	1.0	0.0	1.0	0.9	1.0	1.0	1.0	1.0
39	-49.53	-68.1744	0.9	0.9	0.9	0.9	1.0	1.0	1.0	1.0	1.0	1.0
40	-47.61	-65.7979	1.0	1.0	1.0	1.0	1.0	1.0	1.0	1.0	1.0	1.0
41	-47.94	-66.2073	0.8	0.7	0.8	0.7	1.0	1.0	1.0	1.0	1.0	1.0
42	-46.72	-69.0699	0.8	0.7	0.8	0.7	0.9	0.8	0.9	0.8	0.9	0.9
43	-46.53	-69.401	0.7	0.7	0.7	0.7	0.7	0.7	0.9	0.9	0.9	0.9
44	-48.54	-67.015	0.8	0.8	0.8	0.8	1.0	1.0	1.0	1.0	1.0	1.0
45	-41.14	-69.46	0.0	0.0	0.5	0.3	0.6	0.4	0.6	0.5	0.8	0.5
46	70.47	-52.88	0.5	0.0	0.9	0.0	0.9	0.0	1.0	0.0	1.0	0.0
47	71.36	-24.53	0.6	0.0	0.6	0.0	1.0	0.0	1.0	0.0	1.0	0.0
48	47.6	-111.25	0.5	0.1	0.8	0.1	0.8	0.7	1.0	0.7	1.0	0.9
49	67.87	44.13	1.0	0.0	1.0	0.0	1.0	0.0	1.0	0.0	1.0	0.0
50	60.9987	-138.5294	0.6	0.0	0.7	0.3	0.7	0.3	0.9	0.5	1.0	0.6
51	56.4772	12.9260	0.0	0.0	0.0	0.0	0.9	0.0	1.0	0.6	1.0	0.6
52	-70.7583	11.6444	-	-	-	-	-	-	-	-	-	-
53	63.5059	-51.0454	0.0	0.0	0.5	0.0	1.0	0.2	1.0	1.0	1.0	1.0
54	62.2421	-49.0481	0.4	0.0	0.5	0.0	0.8	0.3	1.0	1.0	1.0	1.0
55	63.5163	-50.9652	0.0	0.0	0.5	0.0	1.0	0.2	1.0	1.0	1.0	1.0
56	65.7621	-51.2866	0.0	0.0	0.6	0.0	0.9	0.0	0.9	0.0	1.0	1.0
57	62.4791	-50.2146	0.5	0.0	0.6	0.0	0.6	0.3	1.0	0.9	1.0	1.0
58	67.359	-52.3693	0.4	0.0	0.5	0.0	1.0	0.0	1.0	0.1	1.0	1.0
59	71.8288	-22.8017	0.0	0.0	1.0	0.0	1.0	0.0	1.0	0.0	1.0	0.0
60	70.4565	-22.2694	0.9	0.0	1.0	0.0	1.0	0.0	1.0	0.0	1.0	0.0
61	78.0407	-21.4572	1.0	0.0	1.0	0.0	1.0	0.0	1.0	0.0	1.0	0.0
62	81.3073	-78.2145	0.0	0.0	0.0	0.0	0.0	0.0	0.9	0.0	1.0	0.0

63	71.8426	-22.7902	0.0	0.0	0.0	0.0	1.0	0.0	1.0	0.0	1.0	0.0
64	72.3906	-25.1555	-99.0	-99.0	-99.0	-99.0	0.3	0.0	0.4	0.0	1.0	0.0

35

Table S5. Number of locations for north and south HLD regions which have SI value above a certain threshold (0.9, 0.8, 0.7, 0.6, 0.5, 0.4) depending on the environment size (30 arcsec, 0.1°, 0.5° and 1°).

No.	lat	lon	at loc.		30 arcsec		0.1°		0.5°		1°	
			max	min	max	min	max	min	max	min	max	min
NORTH HLD REGION (NORTH OF 50°N)												
SI ≥ 0.9			5	0	12	0	27	4	39	16	44	23
SI ≥ 0.8			6	0	14	0	31	4	40	16	46	23
SI ≥ 0.7			8	0	17	0	33	6	42	18	46	24
SI ≥ 0.6			12	0	22	0	36	6	43	19	46	26
SI ≥ 0.5			17	0	27	1	38	7	44	22	48	27
SI ≥ 0.4			20	0	29	1	40	7	46	23	49	27
SOUTH HLD REGION (SOUTH OF 40°S)												
SI ≥ 0.9			3	2	3	2	7	6	10	7	10	9
SI ≥ 0.8			6	3	6	3	9	7	10	10	11	10
SI ≥ 0.7			7	6	9	7	10	10	10	10	11	10
SI ≥ 0.6			7	6	9	8	11	10	11	10	11	10
SI ≥ 0.5			7	6	10	8	11	10	11	11	11	11
SI ≥ 0.4			7	6	10	8	11	11	11	11	11	11

Table S6. Mineralogical and elemental composition of PM2 and PM1000 of soils at Western Siberia.

Proxy	HLD#3 (Podzols)			HLD #5 (Retisols and Gleysols)				HLD #6 (Retisols and Gleysols)				HLD #8 (Phaeozems and Stagnosols)			
	PM2, n=1	PM1000, n=10		PM2, n=4		PM1000, n=7		PM2, n=5		PM1000, n=5		PM2, n=8		PM1000, n=11	
	M	M	SD	M	SD	M	SD	M	SD	M	SD	M	SD	M	SD
Smectite, %	36.7	0.0	0.0	51.5	4.1	13.7	10.4	46.8	5.5	17.7	10.5	47.6	11.6	23.2	8.7
Illite, %	5.5	2.9	1.0	8.7	1.4	9.3	0.8	8.1	0.9	6.3	0.7	8.3	2.2	10.1	1.5
I/Sm, %	23.6	<0.1	-	18.2	1.0	<0.1	-	20.1	5.1	<0.1	-	26.0	10.1	<0.1	-
Kaolinite, %	6.7	1.4	1.2	3.5	0.8	2.3	0.6	6.5	2.5	2.2	1.1	5.3	1.7	3.4	0.7
Chlorite, %	2.1	0.4	0.5	2.4	0.8	1.0	0.7	1.1	1.1	2.1	0.8	1.9	0.5	1.7	0.7
Pls, %	6.4	5.5	2.7	4.3	0.8	15.5	3.2	4.5	0.7	14.6	3.4	3.5	1.3	13.8	2.5
PFS, %	7.1	4.9	3.0	4.9	1.3	8.3	1.9	4.3	0.9	8.3	1.4	5.4	1.8	8.1	1.6
Quartz, %	11.2	84.6	6.8	5.7	1.7	49.8	10.2	7.6	4.5	48.7	8.9	4.1	2.6	38.4	6.2
Calcite, %	0.8	0.4	0.2	1.1	0.2	0.0	0.0	1.0	0.7	0.0	0.0	2.0	2.6	1.4	3.1
TOC, %	n.a.	1.7	3.7	1.0	1.0	4.7	7.3	6.0	4.3	1.8	2.9	2.4	3.1	1.0	1.4
Na_2O, %	0.71	0.54	0.32	0.25	0.14	0.99	0.33	0.19	0.09	1.23	0.26	0.18	0.05	0.87	0.24
MgO, %	1.14	0.13	0.11	1.97	0.22	1.18	0.67	1.73	0.37	1.28	0.29	2.33	0.29	1.75	0.43
Al_2O_3, %	20.7	3.5	2.0	15.6	3.1	10.9	2.8	16.2	2.7	10.9	1.3	17.2	3.3	12.0	1.9
P_2O_5, %	0.34	0.47	0.47	0.34	0.47	0.13	0.07	0.44	0.26	0.16	0.15	0.25	0.21	0.27	0.41

S, %	0.24	0.04	0.02	0.14	0.25	0.09	0.04	0.12	0.15	<0.1	-	0.06	0.07	0.06	0.02
K_2O, %	1.64	1.18	0.54	1.86	0.32	1.74	0.29	1.59	0.17	1.88	0.16	2.50	0.42	2.14	0.26
CaO, %	0.48	0.16	0.07	1.20	0.34	0.75	0.36	1.05	0.47	1.18	0.36	2.32	1.77	1.97	2.00
TiO_2, %	0.92	0.33	0.19	0.71	0.14	1.03	0.04	0.61	0.14	1.00	0.21	0.62	0.11	0.97	0.08
MnO, %	0.29	0.02	0.01	0.10	0.06	0.06	0.04	0.13	0.08	0.10	0.09	0.07	0.04	0.12	0.08
Fe_2O_3, %	9.1	0.5	0.4	8.8	2.2	3.6	2.0	9.2	2.8	4.9	1.2	8.8	1.1	5.3	1.5
V, mg/kg	171	30	17	174	45	123	24	164	35	115	14	168	24	140	16
Cr, mg/kg	754	36	26	298	251	129	20	231	67	144	16	216	96	154	28
Co, mg/kg	62	<10	-	22	4.4	15.3	3.5	26.2	6.4	20	7.5	17	2.1	17	3.8
Ni, mg/kg	182	<10	-	115	45	29	15	85	8.0	32	9.4	90	25	47	11
Cu, mg/kg	59	<10	-	54	5.0	20	5.3	38	10	15	1.5	48	9.9	28	4.5
Zn, mg/kg	180	26	8.1	144	21	50	22	136	25	61	17	126	9.7	75	12
As, mg/kg	15	<10	-	13	2.4	<10	-	14	4.5	<10	-	12	3.2	<10	-
Pb, mg/kg	36	<10	-	32	21	19	5.3	28	7.1	23.3	12	19	3.3	27	5.1

I/Sm – illite-smectite mixed-layer minerals with predomination of illite interlayers, PLs – Plagioclases PFS – potassium feldspars, TOC – total organic carbon. M – mean, n – number of observations, SD – standard deviation

Table S7. Major ions, pH value, dust content (in snow) and deposition rate during winter at HLD sources no 4 and 7.

HLD no	M	SD	Me	min	max	n
No 4						
Dust content, mg/m^2	316	439	112	0	1542	30
NH_4^+, mg / L	0.75	0.98	0.30	0	3.60	43
NO_2^-, mg / L	0.015	0.019	0.008	0	0.08	107
NO_3^-, mg / L	2.3	3.4	1.4	0	20.4	118
pH	6.6	0.8	6.7	4.1	8.4	129
No 7						
Dust deposition rate, mg/m^2/d	1.67	1.67	1.08	0.05	6.6	38
NH_4^+, mg / L	0.20	0.009	0.10	0	1.34	682
NO_2^-, mg / L	0.027	0.007	0	0	0.61	127
NO_3^-, mg / L	0.47	0.02	0.19	0	3.93	697
pH	6.1	0.02	6.1	4.6	8.0	585

M – mean, max – maximum, Me – median, min – minimum, N – number of observations, SD – standard deviation.

Table S8. Some characteristics of tailing ponds on the Kola Peninsula (Masloboev et al., 2016).

No.	Object	Exploitation period	Total area, ha	Resource, mln. t
1	Tailing pond of processing plant no. 1 of the Pechenganickel works, JSC Kola MMC	1945 - 1994	1033	~220
2	Tailing pond of processing plant no. 2 of the Pechenganickel works, JSC Kola MMC	1965 - present time		22.4
3	Tailing pond of processing plant of the Severonikel works, JSC Kola MMC	1935 - 1978	No data	5.3
4	Dumps of granulated slag of the Pechenganickel works, JSC Kola MMC	1945 - present time	80	47
5	Tailing pond No 1 and No 2 of crushing and processing plant, JSC Olkon	1954 - present time	1400	~300
6	Tailing pond of apatite-nepheline processing plant no.1 (ANOF-1), JSC Apatit	1957 - 1963	120	24.4
7	Tailing pond of apatite-nepheline processing plant no. 2 (ANOF-2), JSC Apatit	1963 - present time	1652	~550
8	Tailing pond of apatite-nepheline processing plant no. 3 (ANOF-3), JSC Apatit	1988 - present time	1158	~250
9	Tailing pond of JSC Kovdorskiy GOK, (field no. 1)	1962 -1980	330	53.8
10	Tailing pond of JSC Kovdorskiy GOK, (field no. 2)	1988 - present time	900	80
11	Tailing pond of LLC Lovoserskiy GOK	1951 - present time	No data	12
12	Tailing pond of LLC Kovdorslyuda	1959 - present time	35	6

Supplement: Central part of East European Plain: partitioning elements among five particle size-fractions

Topsoil (0-10 cm) samples were collected along several transects (Samonova et al., 2020) crossing gully and bulka (Fig 1A). The collected bulk samples (n = 22) were physically fractionated into five particle size fractions (1000-250, 250-50, 50-10, 10-1 and <1 μm, n=100). The boundaries between particle size classes were defined in accordance with the Russian conventional fraction groups: coarse and medium sand (1000-250 μm), fine sand (250-50 μm), coarse silt (50-10 μm), medium and fine silt (10-1 μm), clay (<1 μm). The concentrations of Al, Fe, Mn, Ti, Li, Be, Sc, V, Cr, Co, Ni, Cu, Zn, Ga, As, Rb, Mo, Cd, Sn, Sb, Cs, Pb, Ta, Tl, Bi, Th, Y, Nb, Ba, U, Zr, Sr, Hf, were determined on Elan-6100 and Optima-4300 DV spectrometers (Perkin Elmer Inc., USA) by ICP-AES/MS after digestion of samples in a mixture of acids (NSAM-499-AES/MS method). In physical fractionation the sand fractions were separated from the bulk soil samples by wet sieving while the silt fractions, as well as the clay fraction, were obtained by sedimentation and siphoning, during times determined by Stokes' law.

The boundaries between particle size classes were defined in accordance with the Russian conventional fraction groups: coarse and medium sand (1000-250 μm), fine sand (250-50 μm), coarse silt (50-10 μm), medium and fine silt (10-1 μm), clay (<1 μm). The measured concentrations and element distribution among soil particle size fractions are shown in Fig. 2A, Fig. 3A and Fig. 4A. Because of the different ways in which the elements can occur in the soils (Samonova and Aseyeva, 2019) their distribution among particle size fractions varies. However, we observed some common patterns in the partitioning of the elements, which allowed us to arrange them into several distinct groups (group A, group B, and group C). According to our results, the majority of elements (Al, Cd, Zn, Sc, V, Tl, Pb, Rb, Ti, Nb, Th, Y, U, Li, Cs, Be, Ga) show the progressive accumulation from coarser to the finer fractions and a maximum of the element concentration in the clay fraction (Fig.2A). The predominant accumulation of metals in the fine fractions was reported earlier both for the natural and polluted soils (Hardy and Cornu 2006; Ljung et al. 2006) suggesting that these elements are mainly found in the secondary minerals such as phyllosilicate clays, where they occur as structural components or in the form of the adsorbed ions. The further study of the element partitioning showed that group A is not homogeneous because of some differences in the distribution of the elements among the two sand fractions, which allowed to incorporate the elements in several subgroups. In the first subgroup, which includes Al, Cd, Zn, Sc, V, Tl, Pb, Rb, the two sand fractions hosts nearly equal average amounts of the elements, while in the second subgroup (Ti, Nb, Th, Y, U) the finer sand fraction (presumably due to preferential accumulation of stable minerals like rutile, titanite) shows higher concentrations of the elements (especially in case of Ti and Nb). The lithic elements (Li, Cs, Be, Ga), which make up the third subgroup in group A, tend to enrich the coarse sand fraction. The elements from group B in contrast to group A revealed the minimal concentrations not in the sand but in the silt fractions, specifically, in coarse silt fraction (Cr, Ni, Sn, Bi, Sb, As, Mn, Co) or both silt fractions (Fe, Mo), but major element-hosting particle size fraction remained the same (the clay fraction). The majority of the elements that comprise this group participate in redox reactions and

belong to arsenic group or represent typical elements of the ferro-family. The latter group can occur in soil as structural components of primary ferrous minerals or/and as co-precipitates in secondary Fe-Mn (hydr)oxides. Most of the elements from group B do not accumulate in the sand fractions, except for Mn, Co and Mo, which in some cases enrich the sand fraction. Such bimodal distribution with two concentration maxima (one in clay and one in sand) was reported earlier and can be explained by the presence of several hosting minerals and phases having high retention for these metals. In the clay Mn and Co are apparently associated with secondary clay minerals, but in the sand they are likely bound to newly formed Mn (hydr)oxides. The last group (group C) incorporates stable elements Zr and Hf. They reveal the maximum concentrations in the silt fractions, with a maximum in the coarse silt, and minimal concentration in the coarse and medium sand fraction. Such distribution among different particle size fractions can be explained by the occurrence of these elements in detrital grains of primary accessory minerals, such as zircon, usually concentrating in the fine sand to coarse silt fractions. In conclusion, it is worth pointing out that our geochemical study conducted in the central part of European Russia showed that the majority of the elements in topsoil horizons of typical soils (Retisols and Regosols) have common types of distribution among particle size fractions displaying the progressive accumulation in the finer fractions. However, our data also provide the evidence that preferential association of metals with particle size fractions is not limited to the clay fraction. Such elements as Mn, Co tend to have bimodal distribution with concentration maxima in the clay and the sand fraction. The partitioning of Zr and Nb accumulating in the silt fractions is governed by their presence in the mineral structure of accessory minerals that are stable during the processes of transport, physicochemical weathering, and soil formation. The coarse silt fraction, with particle sizes 50-10 μm, in many cases is depleted in elements which can be a result of its loessial origin.

References

Samonova O.A. and Aseyeva E.N.: Particle size partitioning of metals in humus horizons of two small erosional landforms in the middle Protva basin – a comparative study. GEOGRAPHY, ENVIRONMENT, SUSTAINABILITY. 2020;13(1):260-271. https://doi.org/10.24057/2071-9388-2019-116, 2020.

Samonova O. A., Aseyeva E. N., Chernitsova O. V. Data on rare earth elements in different particle size fractions of topsoil for two small erosional landforms in central European Russia. // Data in Brief, 30, pp. 105450, https://doi.org/10.1016/j.dib.2020.105450, 2020.

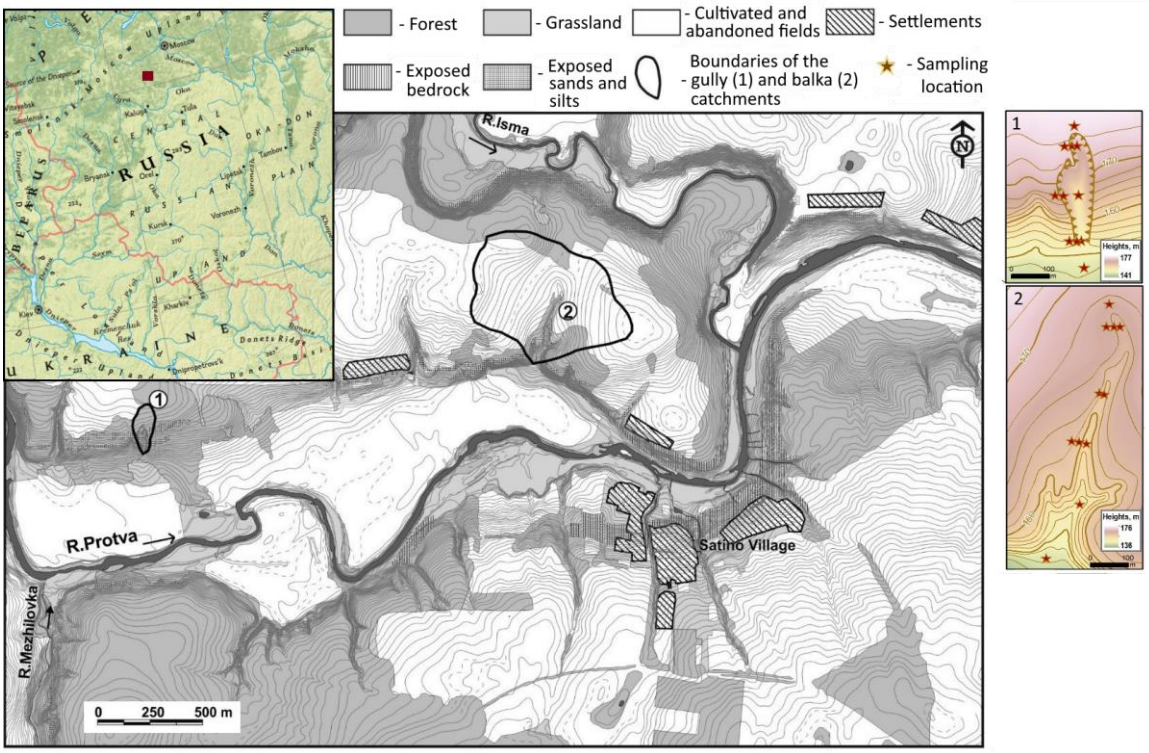

125

Figure S1. The map of the study area in the Central European Russia with the study objects and sampling locations (Samonova and Aseyeva, 2020)

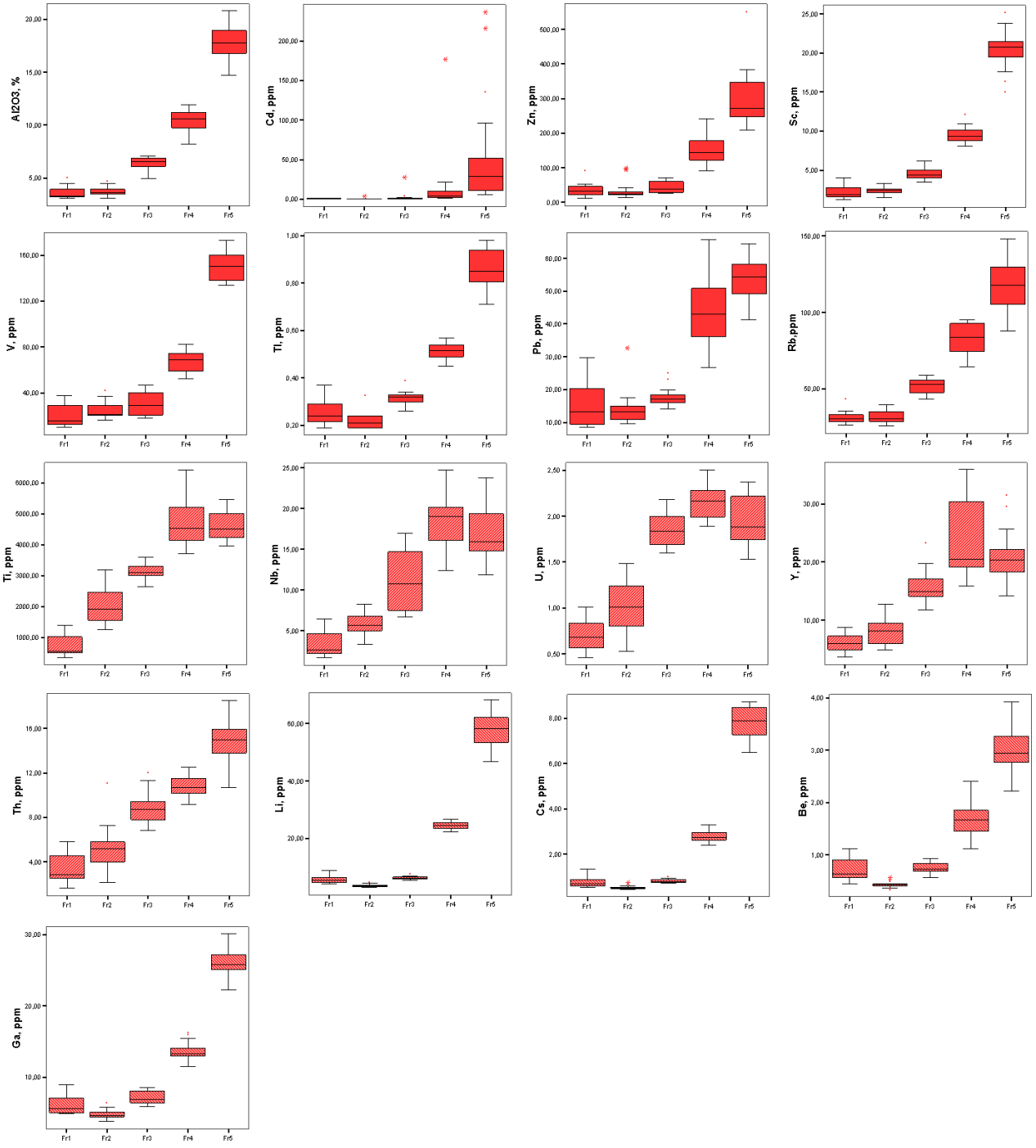

Figure S2. The abundances of elements (group A) in the soil particle size fractions. Median – is indicated as a line across the box. X-axe: particle size fractions Fr1 – coarse and medium sand (1000-250μm); Fr2 – fine sand (250-50μm); Fr3 – coarse silt (50-10μm); Fr4 – medium and fine silt (10-1μm); Fr5 – clay (<1 μm).

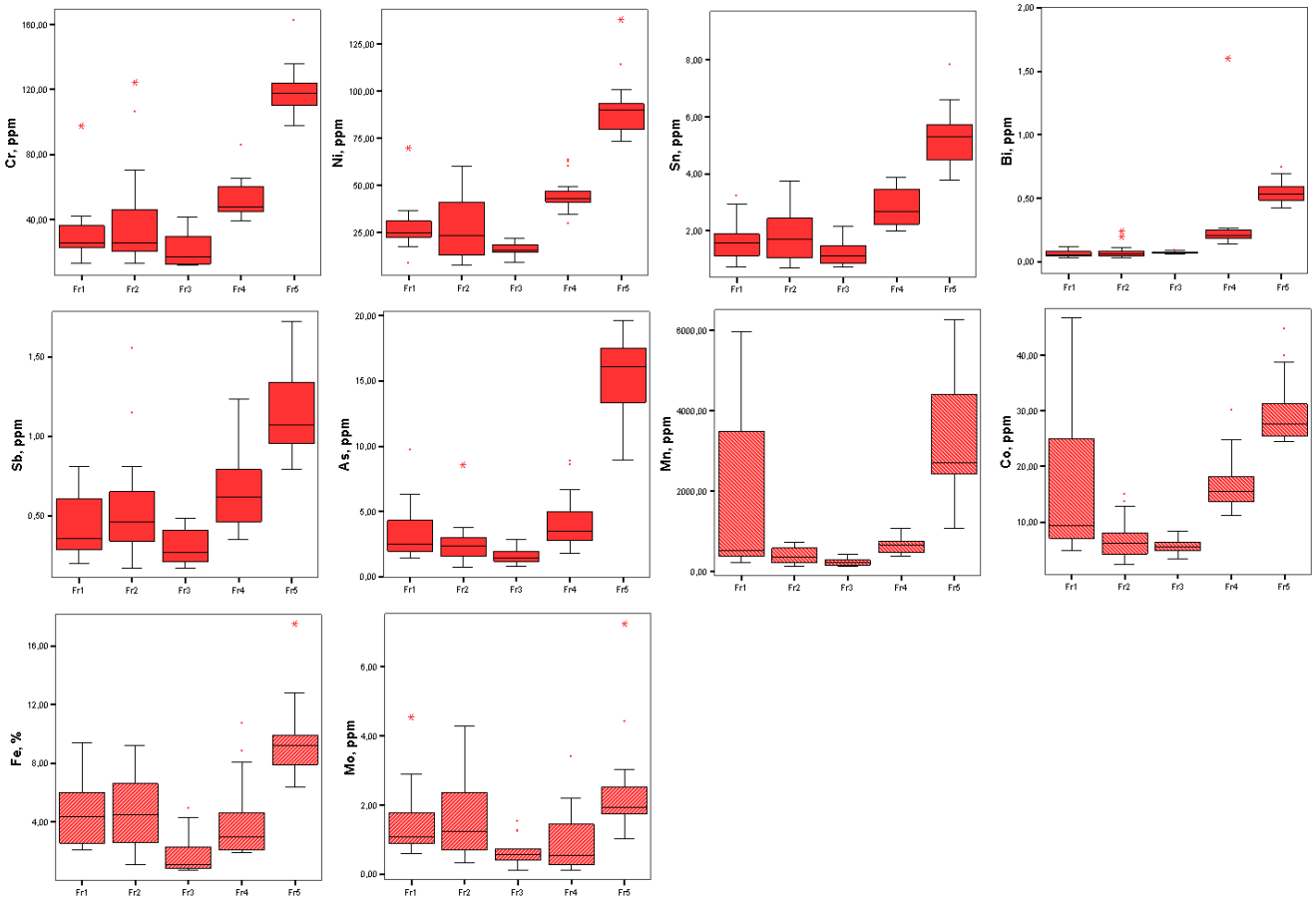

Figure S3. The abundances of elements (group B) in the soil particle size fractions. Median – is indicated as a line across the box. X-axe: particle size fractions Fr1 – coarse and medium sand (1000-250μm); Fr2 – fine sand (250-50μm); Fr3 – coarse silt (50-10μm); Fr4 – medium and fine silt (10-1μm); Fr5 – clay (<1 μm).

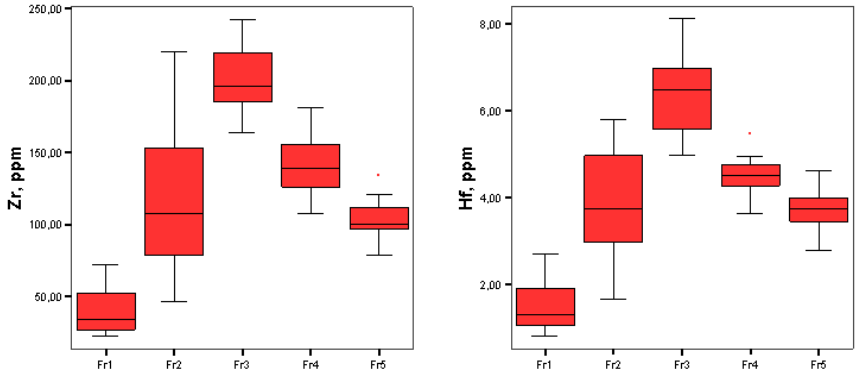

Figure S4. The abundances of elements (group C) in the soil particle size fractions. Median – is indicated as a line across the box. X-axe: particle size fractions Fr1 – coarse and medium sand (1000-250μm); Fr2 – fine sand (250-50μm); Fr3 – coarse silt (50-10μm); Fr4 – medium and fine silt (10-1μm); Fr5 – clay (<1 μm).